

# 2D Magnetotelluric (MT) Modelling for Geothermal System Interpretation

Eko Minarto\*,<sup>1</sup> Mohammad Istajarul Alim,<sup>1</sup> and Ahmad Zarkasy<sup>2</sup>

<sup>1</sup>Department of Physics, Faculty of Science and Analytical Data, Institut Teknologi Sepuluh Nopember, Kampus ITS Sukolilo, Surabaya 60111

<sup>2</sup>Center for Mineral, Coal, and Geothermal Resources, Geological Agency (PSDMBP), Ministry of Energy and Mineral Resources, Jl. Soekarno Hatta No.444, Pasirluyu, Kec. Regol, Kota Bandung, 40254

**Abstract:** Geothermal systems are areas beneath the earth's surface that store circulating heat energy. The heat energy stored in the geothermal system can be utilized by humans as an environmentally friendly alternative energy. Determining the geothermal system area requires geophysical exploration methods that have deep enough penetration and can distinguish soil structures based on the value of resistivity. One method that is effective in determining geothermal systems is the magnetotelluric (MT) method. This method receives electric and magnetic field signals from the induction of subsurface rocks to the electromagnetic wave activity of solar storms and lightning. The signal is then processed to produce a resistivity value. This type of resistance data can then present the structure of the geothermal system, including impermeable rocks, reservoirs and magmatic intrusion zones. This study also collaborated with supporting geological and geochemical data. The results of the magnetotelluric method analysis for the geothermal system of this study area are suspected to have caps rocks with a resistivity of less than 10 m spread near the surface. Reservoirs that have a resistivity of 10-40 m are located at a depth of about 1000 m below the surface based on the interpretation of all data.

Keywords: Electromagnetics; interpretation; magnetotelluric; geothermal systems; caps rocks.

\*Corresponding author: minarto@physics.its.ac.id

<http://dx.doi.org/10.12962/j24604682.v21i3.22613>  
2460-4682 ©Departemen Fisika, FSAD-ITS

## I. INTRODUCTION

Geothermal energy is one of the most attractive resources for exploration. This is because geothermal energy is one of the natural resources without fuel and produces few waste emissions [1]. Geothermal energy is also an alternative energy source that can help provide environmentally friendly energy in the future [2]. Indonesia itself has launched a program to start conducting geothermal exploration on a large scale, considering that Indonesia is a country that has the largest geothermal reserves in the world [3].

A geothermal system can be built from three main components, namely geothermal sources, reservoirs and fluids [4]. The presence or absence of these three components is absolutely necessary in a geothermal system. If one of them is absent, the geothermal system cannot be formed. Reservoirs can be formed from rocks that have high porosity and permeability [5]. However, in order for a geothermal system to produce a system that has a reservoir with a high temperature, there needs to be an additional component, namely a layer of fluid-tight rock [6].

The magnetotelluric geophysical approach is useful for studying geothermal sites because it uses changes in magnetic and electric fields to show how the electrical conductivity of the ground is spread out [7]. These changes in magnetic and electric fields will be detected on the earth's surface using time variations. The interaction between the electric and magnetic fields produces a new value known as impedance (Z). The re-

sultant impedance value can represent the apparent resistivity and phase values at a given measurement site. These numbers can then be utilized to calculate subsurface resistivity using data from the inversion model. Inversion processing is a method for connecting field data to model parameters using the forward modelling function [8].

The magnetotelluric technique will use two fields measured in mutually perpendicular directions. These two fields are measured in the x and y directions, yielding four data points: the magnetic field x, the magnetic field y, the electric field x, and the electric field y. All of this data is significant for collecting impedance information using Maxwell's equations and certain models [9]. The magnetotelluric field data, consisting of magnetic and electric field data, will be translated into the frequency domain to determine the impedance value. The observed magnetic and electric fields are both bidirectional vector quantities; hence, the impedance value is a tensor. The impedance tensor, which can be written as eq. (1) [10], shows how the electric field vector and the magnetic field vector are connected in a straight line.

$$\begin{bmatrix} E_x \\ E_y \end{bmatrix} = \begin{bmatrix} Z_{xx} & Z_{xy} \\ Z_{yx} & Z_{yy} \end{bmatrix} \begin{bmatrix} H_x \\ H_y \end{bmatrix} \quad (1)$$

In the two-dimensional model, there are two modes, namely TE (transverse electric) and TM (transverse magnetic). The TE mode is for an electric field that is parallel to the strike direction so that the magnetic field is perpendicular, while the TM mode is for an electric field that is perpendicular to the

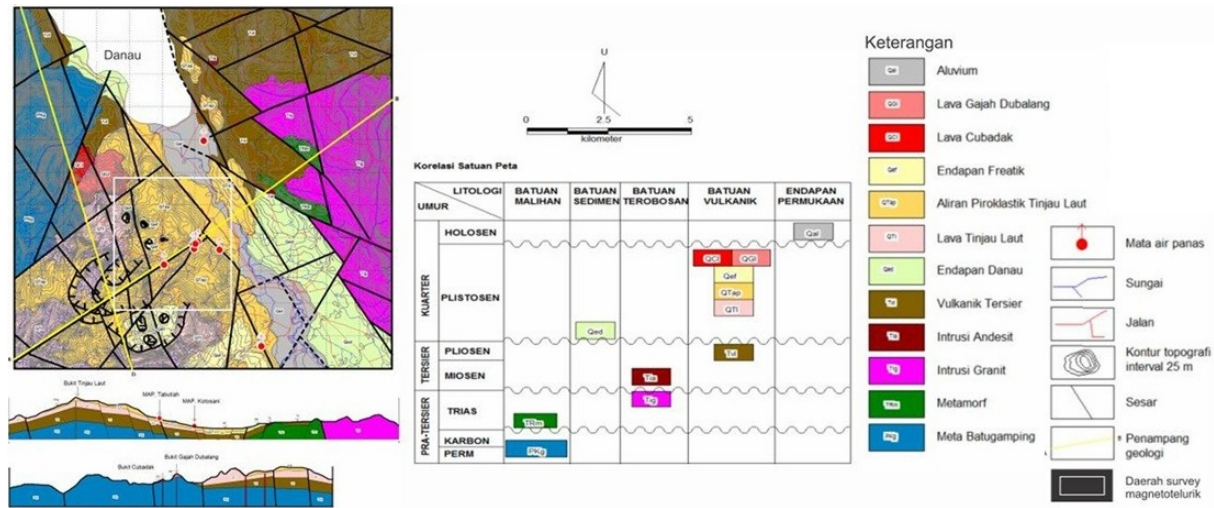
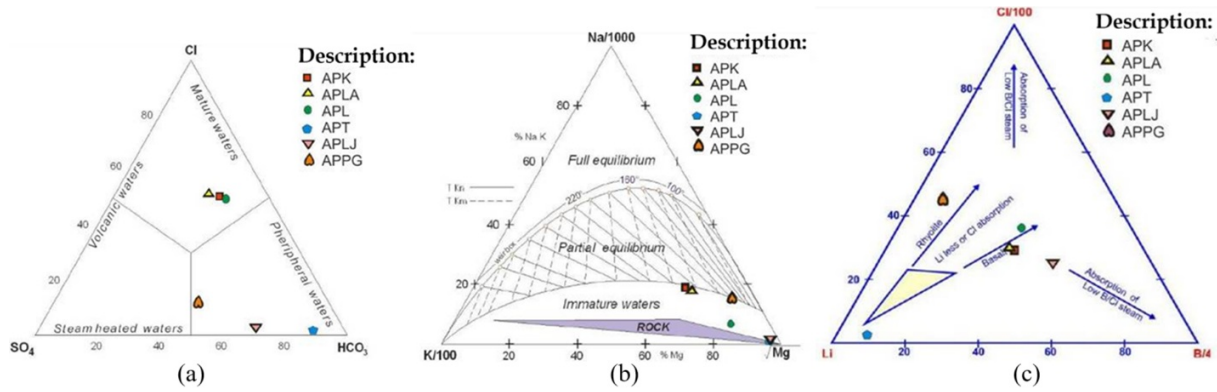


FIG. 1: Regional geological map of the research area [13].

FIG. 2: Trilinear diagrams (a) CL-SO<sub>4</sub>-HCO<sub>3</sub>, (b) Na-K-Mg, and (c) Cl-Li-B.

strike direction so that the magnetic field is parallel [11].

Cases in two-dimensional magnetotelluric modelling algorithms can use the Nonlinear Conjugate Gradient (NLCG) algorithm [12]. NLCG inversion is a two-step process: conjugate gradient and line search. In this case, it is the line search that is nonlinear. The inversion problem in the NLCG algorithm itself works by minimizing the objective function  $\Psi$  in eq.(2).  $\lambda$  is a regulation parameter. The positive matrix  $L$  plays a role in varying the error vector.  $L$  is the matrix of the second derivative operator. When the block model is uniform,  $L_m$  approaches the Laplacian function of the log  $\rho$  function.

$$\psi(m) = (d - F(m))^T V^{-1} (d - F(m)) + \lambda m^T L^T L_m \quad (2)$$

## II. MATERIAL AND METHOD

The research area is located on the island of Sumatra, north of the city of Solok in West Sumatra. The geological map of the research area is spanned by the huge Sumatran structural zone, which generates a depression zone in the center (Fig. 1). Fault structures have been discovered in several research regions, indicating the likelihood of hot springs manifesting on

the surface. This region was developed by a volcanic complex that produced pyroclastic rocks and lava of andesite-basaltite composition. The topography of the study region includes volcanic hills, non-volcanic hills, and plains [13].

Geothermal fluids, which are used as a source of geothermal energy, have distinct constituent compositions at each geothermal location. This material may be examined using geochemistry and represented in a trilinear diagram (Fig. 2). The sample to be tested is a geothermal fluid that erupts in the form of a geyser or remains stagnant on the surface due to fissures or faults, allowing the trapped geothermal fluid to flow through the crack [14]. Previous geochemical research has shown that the fluid coming from the hot springs on the ground around the research site is a mix of chloride and bicarbonate. The APK, APLA, and APL hot springs all include chloride fluids. The hot springs contain bicarbonate. Chloride-dominated hot springs originate straight from reservoirs and do not mingle with surface water. Bicarbonate-type hot springs are those that have been polluted by surface water [15].

The reservoir temperature may be determined based on the sodium, potassium, and magnesium concentration [16]. The

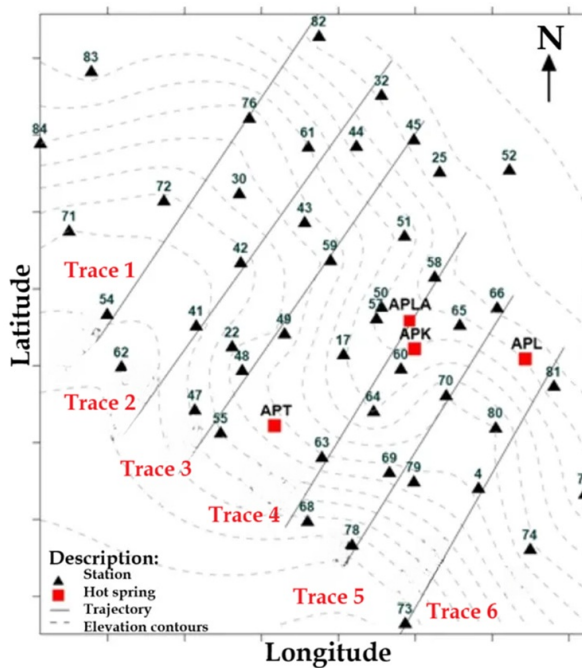


FIG. 3: Magnetotelluric measurement station points, trajectory design, and research area hot springs.

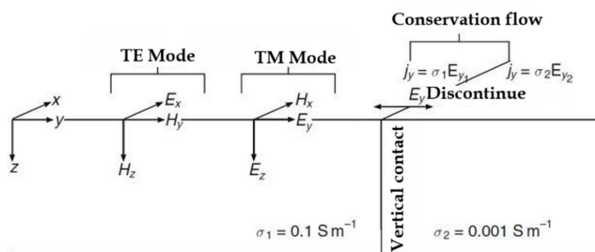


FIG. 4: Transverse electric (TE) and transverse magnetic (TM) modes in vertical contact contrast.

Na-K-Mg figure in the appendix shows that the APK, APLA, and APL hot springs have reservoir temperatures of roughly 200C. The APT, APLJ, and APPG hot springs do not have an estimated reservoir temperature of 200C. The study area is far from the APLJ and APPG hot springs, so there isn't much chance that the reservoirs that feed the hot springs and the heat source will communicate with each other.

This research can be made into a 2-dimensional analysis trajectory of 6 trajectories. The points of the magnetotelluric measurement stations, the trajectory design and the hot spring points can be seen in Fig. 3. This study used magnetotelluric data from the Center for Mineral, Coal, and Geothermal Resources, Geological Agency (PSDMBP) uses two modes measurement in the two-dimensional model, TE (transverse electric) and TM (transverse magnetic) as shown Fig. 4. It comes in the form of 45 measurement points that will be turned into a one-dimensional model and 29 points that will be turned into a two-dimensional model.

The PSDMBP magnetotelluric survey team gathered and

calibrated magnetotelluric raw data. This data needs to be changed from a time domain to a frequency domain using the Fourier transformation method and SSMT2000 software. This is because the information on penetration depth can only be obtained from the frequency value based on the skin depth. To find and get rid of outliers in non-Gaussian noise-skewed data, you also need a strong processing step or a statistically based data processing method that reweights the residuals.

The magnetotelluric data processing then proceeds, utilising MT Editor software to execute the impedance tensor rotation process, which aligns with the geological conditions in the field. At this stage, the xy and yx resistivity curves are also smoothed based on cross power selection. This is because the result of the robust processing only eliminates some of the outliers. As for random noise due to interference during field acquisition, it needs to be done manually at the cross-power selection stage.

Once the resistivity curve has been made smooth using cross-power selection, Winglink software can be used to make a trajectory that will be turned into a two-dimensional model and pick which points will be used as parameters for the two-dimensional inversion. Then the next stage can be continued for the analysis of all measurement points of the work results using MT Editor software. This analysis aims to smooth the cross-power selection result curve when the best solution cannot be found mathematically. The method used at this stage is to remove noise data at a frequency to obtain the best solution.

The smoothing stage in this study uses the D+ method. The D+ method is a geophysical data processing technique, specifically for electrical resistivity sounding data, which aims to ensure physically valid data responses that approximate a one-dimensional (1D) model. This method is also used to examine the causal relationship between apparent resistivity and phase curves, as well as to obtain interpolation points that replace points omitted during processing. The smoothing curve and measurement data for each frequency for the resistivity part are maintained so that the error value is less than 5%. As for the phase part, 5% or 10% is used for the error value. For measurement points with a good phase curve trend, use 5%; for those without, 10% [17].

This study also uses static shift effect correction. Ideally, the TE and TM curves in magnetotellurics will overlap, but for some reason they may not, so it is necessary to correct for the static shift effect [18]. In this study, the method used is the median average approach. This method looks at the response between all measurement stations and then a smoothing process is carried out on a surface frequency [19]. If the static shift effect has been corrected correctly, it can be continued for a 1-dimensional sounding analysis and ends in a 2-dimensional model inversion so that the resistivity cross-section of each trajectory is obtained. The results of 2D resistivity modelling employing magnetotelluric geophysical techniques, as well as geological and geochemical studies, must be consistently compared across the three data sets. When these three data sets are compared, they are able to detect subsurface characteristics in geothermal systems and determine the kind of geothermal fluid manifestation.



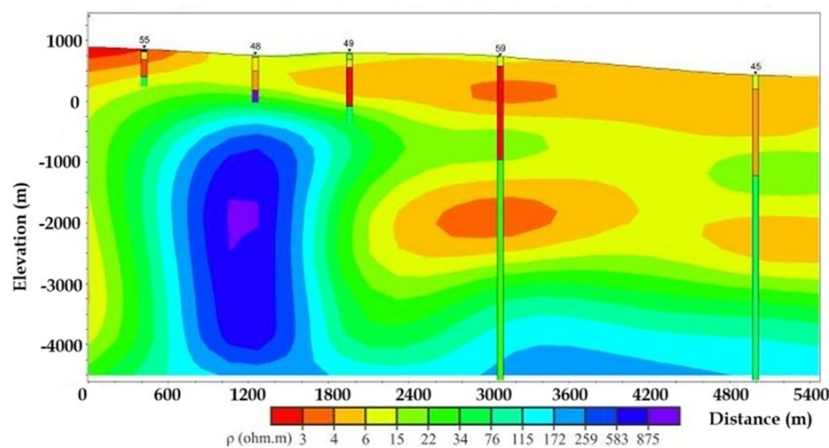


FIG. 5: The result of the 2-dimensional model of the 1-dimensional inversion interpolation on the 3rd trajectory.

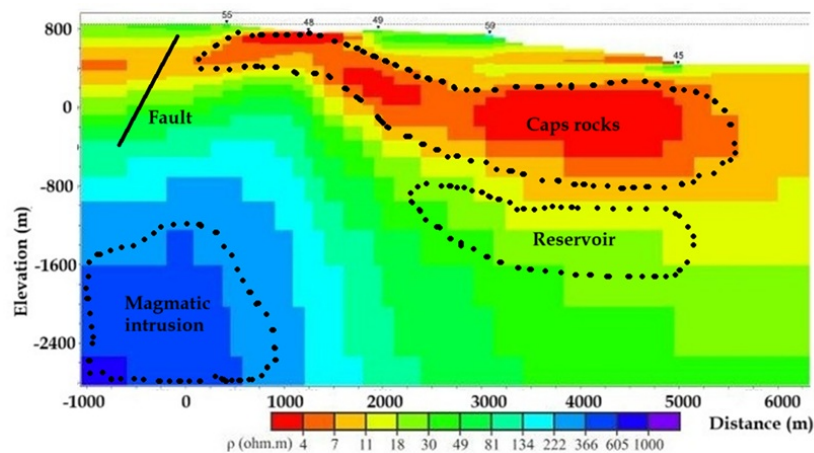


FIG. 6: The result of the 2-dimensional inversion model on trajectory 3.

### III. RESULT AND DISCUSSION

Basically, the natural electromagnetic waves measured on magnetotelluric equipment are affected by various disturbances. Measurement disturbances can be caused by human activity or lightning around the measurement location. As a result, the data recorded on the magnetotelluric equipment will experience chaos at several frequencies. The method of eliminating these disturbance data can be done by cross power selection. The cross-power selection stage is one of the stages in magnetotelluric data processing to obtain better curve results and less natural and artificial noise interference. In theory, the apparent resistivity curve and magnetotelluric phase should be smooth and have relatively gentle curves that rise and fall. To achieve this condition, it is necessary to turn off some data at each frequency of the resistivity and phase curves. The better curve results will, of course, have an effect on the modeling that will be carried out. The number of cross powers used in this study has been set to a maximum of 20. This means that in a frequency there will be a maximum of 20 random data that can be turned off or on again. How-

ever, the smaller the frequency displayed, the less data it will have. Remember that the smaller the frequency, the greater the time period required. So, at the same measurement time, high-frequency data will sample more than low-frequency data.

In this study, the frequency recorded on the magnetotelluric device is in the range of 320 to around 0.001 Hz. However, for the lowest frequency, it is made to be a minimum of 0.01 Hz. This was done because the data below 0.01 records very little data so that the displayed cross power is also very minimal, as explained previously. As a result of these efforts, the depth penetration of the model will certainly be reduced. However, this will not have much impact, considering that based on previous geological research information and the results of rough calculations of the skin depth concept, the depth of the geothermal system reservoir is still within the frequency range used.

This study's static shift makes use of the median average idea. All measurement points in the investigation were recorded at a frequency of 320 Hz as a reference for adjustment. According to the computations, the median value for the xy curve is 16  $\Omega.m$ , whereas the yx curve is 15.5  $\Omega.m$ .

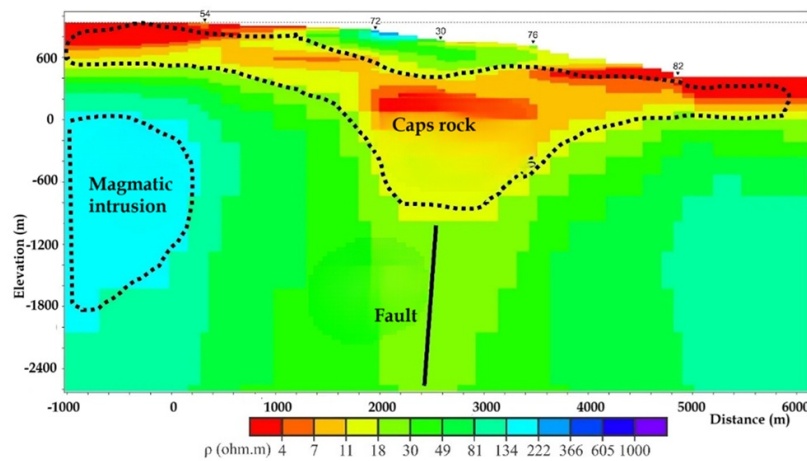


FIG. 7: The result of the 2-dimensional inversion model on trajectory 1.

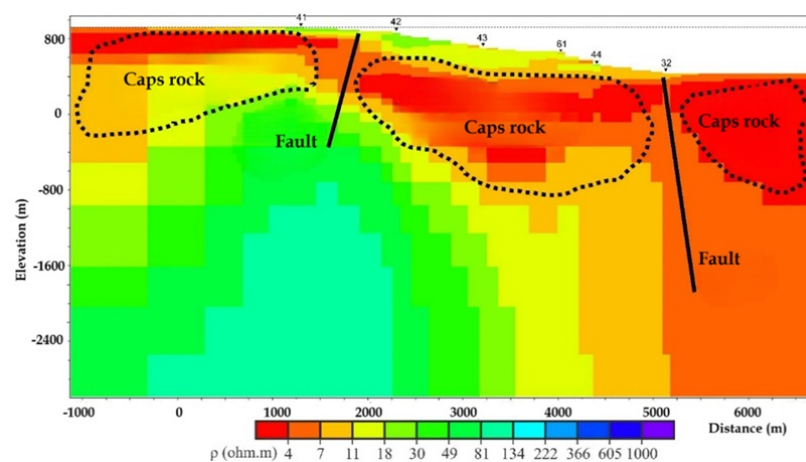


FIG. 8: The result of the 2-dimensional inversion model on trajectory 2.

The average of the two readings is  $15.75 \Omega.m$ . All points in this research are then moved for the apparent resistivity curve at 320 Hz, including the xy and yx curves, to  $15.75 \Omega.m$ . Correction of static shift is very useful in the modeling that will be done later. Mostly, static shifts are caused by heterogeneity of rocks on the surface. The apparent resistivity curve will then experience a vertical shift.

One-dimensional modeling serves as a comparison or controller for two-dimensional modeling. In this investigation, the invariant mode model was applied. The apparent and phase resistivity curves show a mix of TE and TM modes. The algorithm used for one-dimensional inversion modeling is Occam's inversion. This program generates a model that will automatically develop a model using skin depth data. Fig. 5 shows the one-dimensional interpolation model for trajectory 3.

In 2-dimensional modeling, the resistivity varies in the vertical and horizontal dimensions. This study's 2-dimensional inversion modeling is identical to 1-dimensional modeling; however, it only uses the invariant mode. The 1-dimensional

modeling information with interpolation for trajectory 3 reveals that the high resistivity distribution is located on the model's left side, as indicated by the blue color. As a controller, these data must be coupled with two-dimensional inversion modeling. Fig. 6 shows the results of the two-dimensional inversion model on trajectory 3.

The findings of the 2D resistivity cross-section and geochemical study show that in cross-section 1 (Fig. 7), caprocks cover the whole surface region classified as having low resistivity. The middle of the cross-section has an anomaly in the form of a lower resistivity area than the sections to the right and left. This look has also been seen to create a zone that extends to a depth of 2600 m below the sea surface. This type of oddity is considered a defect. Geological evidence corroborates this scenario, since it connects a fault running almost north-south in the center of trajectory 1. The left side of track 1 has a high resistivity value. This situation is assumed to be a magmatic intrusion zone.

Then, on track 2, the left section is still dominated by high resistivity rocks, while the right portion is mostly populated

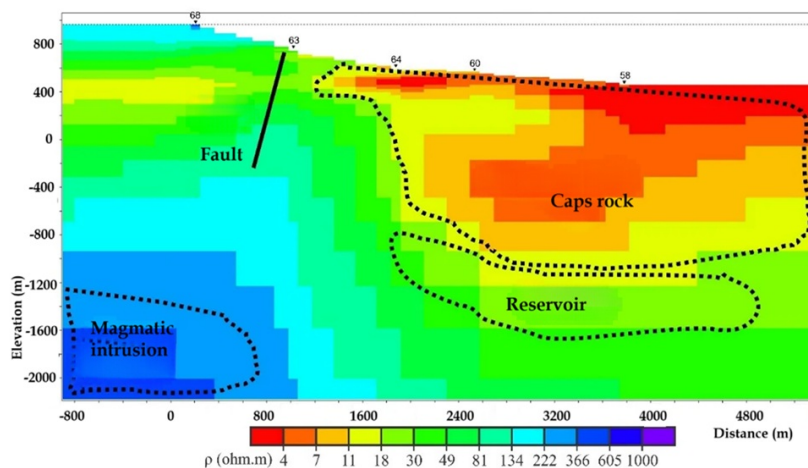


FIG. 9: The result of the 2-dimensional inversion model on trajectory 4.

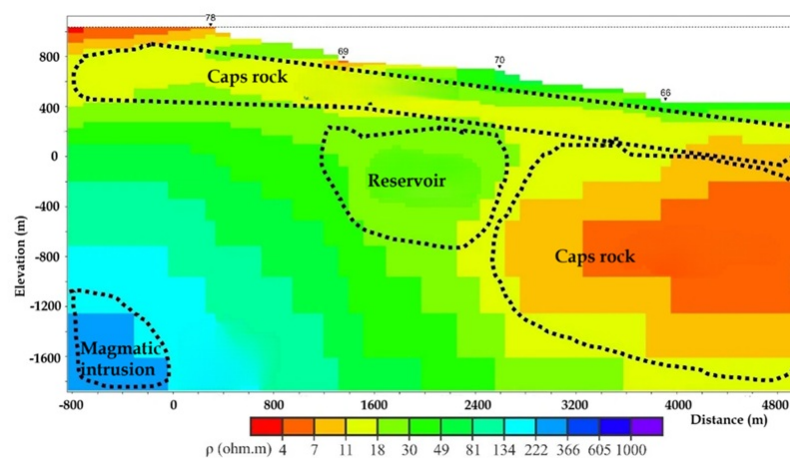


FIG. 10: The result of the 2-dimensional inversion model on trajectory 5.

with low resistivity rocks (Fig. 8). The surface is further distinguished by a layer of low resistivity. However, closer investigation reveals a discontinuity in resistivity on the surface, dividing the layer into three sections. The discontinuity is assumed to represent two fault structures that separate the stratum into three sections. The layer in issue is described as a caprock that encompasses the full surface distribution of Trajectory 2. However, based on geological data, Trajectory 2 follows a path that crosses two faults that run approximately northwest-southeast.

The scenario is different on the third path. On this path, the geological conditions become more complicated, with zones of very high to low resistivity. On the surface, the appearance is defined by a low resistivity distribution, which is assumed to represent a layer of cap rock. Resistivity discontinuity occurs on the left side of the cap rock layer. The discontinuity is thought to be a fault zone that, according to geological data, is spanned by a fault that runs about northwest-southeast. At the bottom of the caprock layer, near the center of the trajectory, there is assumed to be a reservoir of heated geothermal

water-bearing rock. The reservoir zone is distinguished by intermediate resistivity and is caught between zones of high and low resistivity. The reservoir zone on track 3 is adjacent to the APT hot springs, which are most likely influenced by the reservoir's existence. Then, on the left side of track 3's bottom, there is a zone with extremely high resistivity. This location is thought to be quite near to the magma chamber activity of a heat controller that undergoes thermal transfer.

On trajectory 4, there is a zone of low resistivity on the right side near the surface (Fig. 9). This zone is assumed to be a caprock in the form of an impervious layer. Trajectory 4 is crossed by a probable fault on the left side near the surface. The APK and APLA hot springs intersect the route in the center. Based on this information, it is probable that this location has a reservoir zone at the bottom of the extended caprock layer, surrounded by rocks with high resistivity that are thought to represent magmatic intrusion zones.

Continuing on track 5, this area has a relatively thin layer of low resistivity that extends over the surface area as shown in Fig. 10. A low resistivity zone is also found on the right side

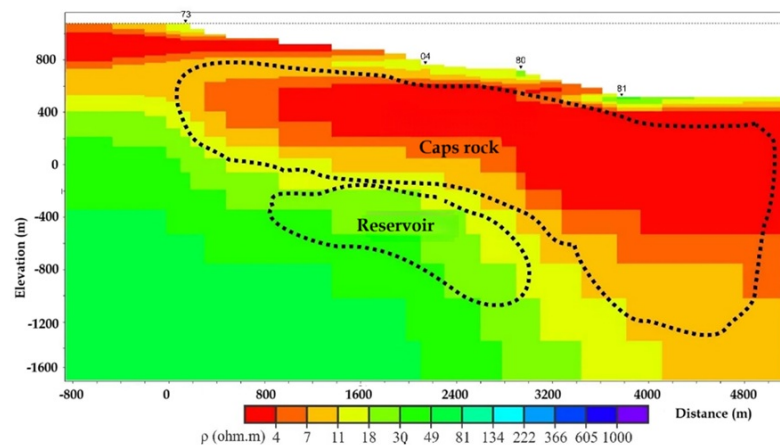


FIG. 11: The result of the 2-dimensional inversion model on trajectory 6.

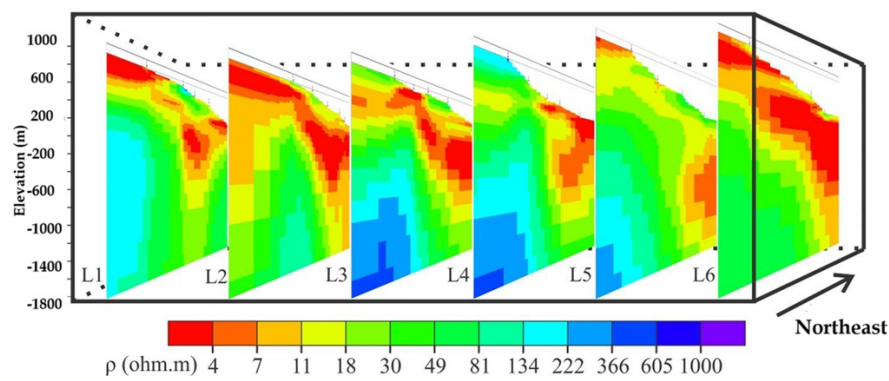


FIG. 12: The 2-dimensional inversion model of the entire research trajectory.

of the track. The thin layer is thought to be a cap rock close to the surface. At the bottom of the cap rock, there is thought to be a relatively large reservoir zone characterized by a moderate resistivity value. The reservoir area is located on the south side of the APK and APLA hot springs and southwest of the APL hot springs. The magmatic intrusion zone on the left side of the transect is characterized by a high resistivity value, like most other transects.

The last track, track 6, runs along the south side of the research area. On this track, the zone with low resistivity is located around the surface (Fig. 11). This zone appears solid with a relatively high thickness, which is thought to be a layer of cap rock. The lower part of this cap layer is thought to have reservoir rock, which, according to the map, is in the southern part of the APK, APLA, and APL hot springs.

Fig. 12 shows all two-dimensional models of the produced all trajectories. The magmatic intrusion zone was discovered in the western section of the geothermal systems study area at varying depths of approximately 2400 m - 2800 m from the surface, and it is distinguished by its high resistivity value.

#### IV. CONCLUSION

The magmatic intrusion zone was discovered in the western section of the geothermal systems study area, and it is distinguished by its high resistivity value. The cap layer has a resistance of less than 10  $\Omega.m$  and spreads close to the surface. The reservoir zone, which has a moderate resistivity value of 10 to 40  $\Omega.m$ , is located in the southern section, near the APK, APLA, and APL hot springs. The reservoir peak is estimated to be roughly 1000 meters below the surface. The results of this study will certainly be very useful in further research for the next stage. Determining the size and depth of the geothermal source for the purposes of exploration and exploitation of existing geothermal sources.

#### Acknowledgments

The author would like to thank the Center for Mineral, Coal, and Geothermal Resources, Geological Agency (PS-DMBP), which has provided data for this research.

- 
- [1] W.E. Glassley, "Geothermal Energy", 0 ed. CRC Press, 2010. doi: 10.1201/EBK1420075700.
- [2] H.K. Gupta, S. Roy, and H.K. Gupta, Eds., "Geothermal energy: an alternative resource for the 21st century", 1st ed. Amsterdam, the Netherlands Boston: Elsevier, 2007.
- [3] Stanford University, Ed., "43rd Workshop on Geothermal Reservoir Engineering 2018", Stanford, California, USA, 12-14 February 2018. in SGP-TR Stanford Geothermal Program workshop report, no. 213. Red Hook, NY: Curran Associates, Inc, 2019.
- [4] M.H. Dickson and UNESCO, Eds., "Geothermal energy: utilization and technology. in Renewable energies series", Paris: UNESCO, 2003.
- [5] E. Minarto, "Pemodelan Inversi Data Geolistrik untuk Menentukan Struktur Perlapisan Bawah Permukaan Daerah Panas-bumi Mataloko," JFA, vol. 3, no. 2, p. 070201, Jun. 2007, doi: 10.12962/j24604682.v3i2.993.
- [6] Y. Wu, and P. Li, "The potential of coupled carbon storage and geothermal extraction in a CO<sub>2</sub>-enhanced geothermal system: a review," Geotherm Energy, vol. 8, no. 1, p. 19, Dec. 2020, doi: 10.1186/s40517-020-00173-w.
- [7] F.J. Esparza and E. GmezTrebio, "On: The magnetotelluric method in the exploration of sedimentary basins," by K. Vozoff (February 1972 G EOPHYSICS, 37, p. 98-141), GEOPHYSICS, vol. 62, no. 2, p. 691-692, Mar. 1997, doi: 10.1190/1.1444178.
- [8] W. Rodi, and R.L. Mackie, "Nonlinear conjugate gradients algorithm for 2-D magnetotelluric inversion," GEOPHYSICS, vol. 66, no. 1, p. 174-187, Jan. 2001, doi: 10.1190/1.1444893.
- [9] A.D. Chave, and A.G. Jones, Eds., "The Magnetotelluric Method: Theory and Practice", 1st ed. Cambridge University Press, 2012. doi: 10.1017/CBO9781139020138.
- [10] M.N. Berdichevski, and V.I. Dmitriev, "Models and methods of magnetotellurics", Berlin: Springer, 2008.
- [11] F. Simpson, and K. Bahr, "Practical Magnetotellurics", 1st ed. Cambridge University Press, 2005. doi: 10.1017/CBO9780511614095.
- [12] G.A. Newman, and D.L. Alumbaugh, "Three-dimensional magnetotelluric inversion using non-linear conjugate gradients," Geophysical Journal International, vol. 140, no. 2, p. 410-424, Feb. 2000, doi: 10.1046/j.1365-246x.2000.00007.x.
- [13] D. Hermawan, and Y. Rezky, "Delineasi daerah prospek panas bumi berdasarkan analisis kelurusan citra landsat di candi umbul - telomoyo, provinsi jawa tengah, buletin sdg, vol. 6, no. 1, p. 1-10, May 2011, doi: 10.47599/bsdg.v6i1.92.
- [14] K. Nicholson, "Geothermal fluids: chemistry and exploration techniques", Berlin: Springer, 2012.
- [15] A.S. Rybak, et al, "Characterization of cyanobacterial mats from an artificial hot spring in Uniejw (Poland) and the potential use of their biomass," Algal Research, vol. 82, p. 103646, Aug. 2024, doi: 10.1016/j.algal.2024.103646.
- [16] A. Satter, and G.M. Iqbal, "Reservoir fluid properties," in Reservoir Engineering, Elsevier, 2016, p. 81-105. doi: 10.1016/B978-0-12-800219-3.00004-8.
- [17] B. Zhou, and T. Dahlin, "Properties and effects of measurement errors on 2D resistivity imaging surveying," Near Surface Geophysics, vol. 1, no. 3, p. 105-117, Aug. 2003, doi: 10.3997/1873-0604.2003001.
- [18] K. Zhang, W. Wei, Q. Lu, H. Wang, and Y. Zhang, "Correction of magnetotelluric static shift by analysis of 3D forward modelling and measured test data," Exploration Geophysics, vol. 47, no. 2, p. 100-107, Jun. 2016, doi: 10.1071/EG14044.
- [19] D. Khan, and R. Burdzik, "Measurement and analysis of transport noise and vibration: A review of techniques, case studies, and future directions," Measurement, vol. 220, p. 113354, Oct. 2023, doi: 10.1016/j.measurement.2023.113354.